AXIAL RESOLUTION ENHACEMENT OF LIGHT-SHEET MICROSCOPY VIA TWO LIGHT-SHEETS

Vannhu Le,[*] Minhnghia Pham, Vandang Hoang

Le Quy Don Technical University, 236 Hoang Quoc Viet Street, Hanoi, Vietnam

[*]*Email: levannhuktq@gmail.com*

Abstract—**Light-sheet fluorescence microscopy has many advantages including high-speed, noninvasive and low photobleaching and photodamage. The light-sheet thickness of light-sheet microscopy is used to determine the axial resolution. However, the light-sheet thickness is limited by the light diffraction. In order to beyond this limit, inhere, we introduce a novel way based on the use of two light-sheets to achieve the enhancement of the axial resolution of light-sheet microscopy. Two images are captured by using both Gaussian light-sheet and negative light-sheet beams. From these two images, a new relationship between them is built to achieve the axial resolution image higher than the image of Gaussian light-sheet. Experimental result is performed, indicating that the effectiveness of the proposed method is better than traditional light-sheet microscopy.**

Keywords: Light-sheet microscopy, super-resolution, fluorescence microscopy.

I. INTRODUCTION

Three dimensional live imaging is a strong tool for good knowledge with the nature of the biological processes. Some 3D imaging techniques have been applied in practical microscopy systems, such as the confocal fluorescence microscopy, the wide-field fluorescence microscopy and the light-sheet microscopy (LSM). While, LSM has been rapidly developed in recent years because this technique is some remarkable advantages such as high-speed, noninvasive and has low photobleaching and photodamage [1-3]. In LSM, the background-noise in the out-of-focus plane is removed by using both illumination lens and detection lens whose optical axes are orthogonal to each other. The thin light-sheet is employed to activate the sample from one outside. The in-of-focus plane of the detection lens should replace the overlap with the active light-sheet, which generates the sharp image. LSM has some advantages as follow: (1) effective optical sectioning capability can reduce the out-of-focus fluorescence background; (2) it has the high imaging speed as the same wide-field microscopy; (3) there are both quite low photo-bleaching and photo-damage; (4) the axial resolution is improved because the axial resolution is determined by the light-sheet thickness which is ultimately limited by light diffraction [4]. While, the lateral resolution of other 3D imaging techniques is better than that of LSM because the lateral resolution of the LSM is determined by the detection object which the number aperture (NA) of detection objective is usually small [4]. To overcome limit, several methods based on the combination of many light-sheets have been introduced, such as, dual-view inverted selective plane illumination microscope (DILSM) [5], STED LSM [6-8], RESOLFT LSM [9], SIM LSM [10-13], Multi SIM LSM (MSIM LSM) [14], multi-views LSM [15-17] and so on.

In STED LSM, there are two light-sheets used for improvement of axial resolution or imaging performance. Two light-sheets which include an ordinary pump beam light-sheet and a doughnut-shaped simulated light-sheet are simultaneously activated into the sample. A smaller light-sheet can be generated by choosing the match between both the pump light-sheet and the simulated light-sheet. The imaging speed of this method is the same as then conventional LSM. However, the sample can be damaged because the high power of laser is required. For double inverter LSM (DiLSM), two images obtained by alternating detection and excitation between the two objectives and then a digital processing is proposed to obtain the higher resolution image. The resulting DiLSM provides isotropic spatial resolution. This method is improved additionally other direction resolution compared the conventional LSM. The imaging speed of this method is slower than the conventional LSM.

There are two methods for achieving the improvement of the axial resolution of LSM by employing three light-sheets, such as SIM and RESOLFT. References [10-13] shown to perform SIM with three light-sheets. For RESOLFT LSM [9], the three light-sheets are applied to increase the axial resolution. In this method, the Gaussian beam is employed twice, while other light-sheet is introduced by using a phase mask, 0-pi. The first step, the Gaussian light-sheet is used to activate the sample. Only the activated sample parts are switched from their initial basic state to the on state. Next step, the phase mask, 0-pi, is used to generate a light-sheet, which features a central zero-intensity plane, switches off the activated sample outside the detection focal plane (above and below). Only fluorophores on the central zero-intensity plane remain activated. Finally step, these can be read out by using the Gaussian light-sheet. For SIM LSM, there are two methods to perform this. First, three SIM light-sheets are generated. Three images are captured by these three SIM light-sheets. The digital processing with these three images is used to the final image. The second, only one SIM light-sheet is generated, the sample is shifted to obtain three images. After three images obtained, the digital processing is used to obtain the final images. The imaging speed of these two methods are lower than then conventional LSM.

It is clear that we can be divided the above methods on two types: the nonlinear processing with many light-sheets (such as

STED LSM, RESOFLT LSM) and the digital processing with many light-sheets (such as SIM SLM, MSIM LSM, multi-view LSM). In this paper, we introduce a novel way based on employing two light-sheets to obtain the enhancement of the axial resolution of LSM. A light-sheet is created by using Gaussian beam and other light-sheet is introduced by using a phase mask 0-pi. From two images captured of these two light-sheets, a new relationship between the two images is built to improve the axial resolution of LSM. Compared with STED LSM and the proposed method, the STED LSM requires a high power in the negative light-sheet. In comparison to DiLSM, the proposed method is simple and can be easy performed.

II. METHOD

In order to obtain two images for the proposed method, the optical system should be two paths in illumination part. A path is corresponding to the Gaussian beam, which is called Gaussian light-sheet (this path is corresponding to traditional LSM) and other path is added a phase mask 0-π, this phase mask is shown in Fig. 1(c), which is called the negative light-sheet.

By using these two light-sheets, the two images can be obtained with two different light sheets. As Figs. 1(a) and 1(b) show, we depict two feasible optical layouts for our method. The first method, when we use the transmitted spatial light modulator (SLM) as shown in Fig. 1(a). In the case, it can be seen that there are two separated illumination paths before the beam splitter (BS): one path is responding to the Gaussian light-sheet, the other path is used to generate the negative light-sheet. Note that the negative light-sheet is generated by using a phase mask 0-π as shown in Fig. 1(c). For the imaging layout, we need to adjust the two illumination paths carefully, to ensure that both Gaussian light-sheet and negative light-sheet are placed in the same position on the sample. Other imaging layout as shown in Fig. 1(b), when the reflective SML is used in the imaging system. In this case, The SLM is employed to switch between 0 phase mask and 0–π phase mask which are responding to generate both the Gaussian light-sheet and the negative light-sheet, respectively.
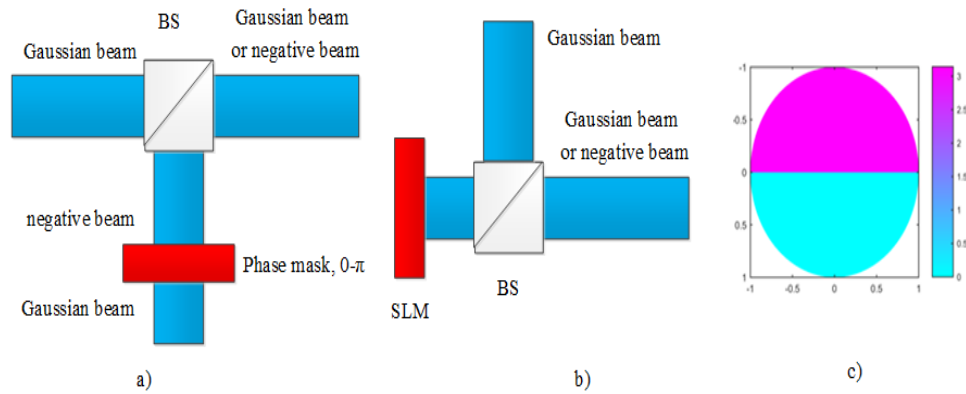

Fig. 1 Two models for generation of both light-sheets and phase mask 0-π, beam splitter (BS).

By multiplying the PSF of the illumination lens and the PSF of the detection lens, the overall-system point spread function (PSF) can be obtained and can be represented by,

$$h_{sys}(x,y,z) = h_{ill}(x,y,z) \times h_{det}(x,y,z)$$
(1)

where $h_{sys}(x,y,z)$, $h_{ill}(x,y,z)$, $h_{det}(x,y,z)$ are the PSF of the overall system, the PSF of the illumination lens and the PSF of the detection lens, respectively. z axis is the detection axis and y axis is the illumination axis.

The recorded image of LSM can be presented by,

$$I(x,y,z) = h_{Sys}(x,y,z) * o(x,y,z)$$
(2)

where $I(x,y,z)$ is the fluorescent signals; $o(x,y,z)$ is the fluorescent sample; $*$.is convolution operator.

When the fluorescent signals excited by both Gaussian and negative light-sheet, the two images are obtained. Here, we propose the new combination between the two images by a relationship as shown in equation (3) in order to obtain the enhancement of the axial resolution,

$$I_{Comb}(x,y,z) = I_{Gaussian}(x,y,z) - \alpha \times \sqrt{I_{Gaussian}(x,y,z) \times I_{negative}(x,y,z)}$$
(3)

where $I_{Gaussian}(x,y,z)$, $I_{negative}(x,y,z)$ are images of the Gaussian light-sheet, and the negative light-sheet, respectively; the coefficient α is the subtraction parameter. This relationship is called the subtraction LSFM.

III. EXPERIMENTAL RERULT

We show the optical configuration to perform the experimental result in this paper. The optical configuration of the imaging system is indicated in Fig.2. The 647nm CW laser source (Coherent, 120mW) is used. The laser beam is collimated by lens L1 and, then this beam is projected onto $\lambda/2$ polarization plate. After passing through the $\lambda/2$ polarization plate, the beam is reflected by using the BS. The reflected beam is projected onto the SLM and the SLM is employed to control the phase mask which is corresponding to each light beam. The phase-modulated beam is reflected back to the beam splitter and passes through it. Then the light beam is reflected by the mirror, which changes the direction of the light beam by 90°. Then, the light beam passes through both lenses (L2 and L3) in order to expand the beam and then a cylindrical lens (L4) is employed to crease the light-sheet. The focal length of lens (L5) is chosen to nearly match the back focal length of the cylindrical lens (L4) in order to avoid the change of the light beam diameter. The light-sheet is used to image into the sample-chamber after passing through an imaging system including the lens (L5), a beam expander (L6 and L7) and the illumination objective (L8, 10X, 0.25). The M2 is used to make the direction-change of the light beam. The fluorescence emitted from the sample is imaged onto the detector by an imaging system in the direction perpendicular to the illumination optical axis including the detection objective (L9, 20X, 0.3) and a tube lens (L10). In our configuration, the sample is moved along z axis by using a motor.

Sample preparation with 1μm diameter fluorescent particles: Embed 1μm diameter fluorescent particles in 1.5% low-melting-point agarose, Type-VII, Sigma-Aldrich, in a custom-made glass capillary (1.5mm inner diameter, 20mm length). Then, extrude the fully gelled agarose from the capillary until the part containing fluorescence particles are completely exposed outside the glass.
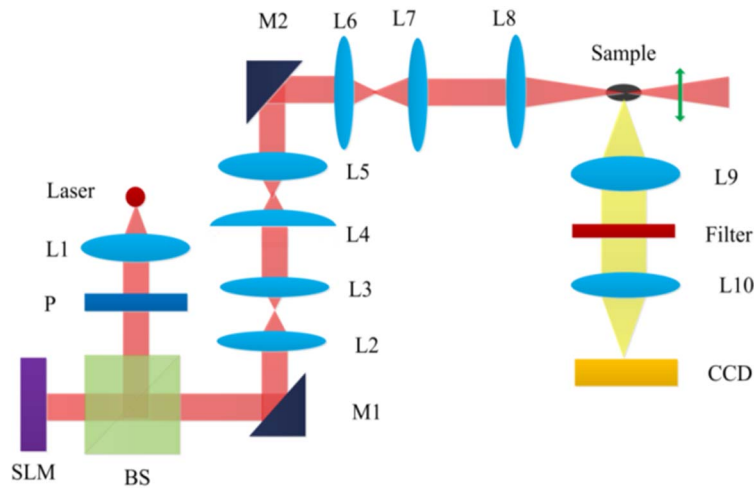

Fig. 2 The configuration of optical system.

The imaging performances of the traditional and subtraction LSFM are performed with 1μm fluorescent particles. A piezo stage is employed to control the sample-shift. The moving step along z axis is set to 0.5μm. At each axial position, the camera captured the fluorescence sequentially. The fluorescence image of each slice is captured by wide field microscopy. The first, we obtain 3D image by using the Gaussian light sheet when LSM is corresponding to 0 phase mask. This 3D image is called the traditional image. Next, we obtian 3D image by using negative light sheet when LSM is corresponding to 0–π phase mask. This 3D image is called the negative image. The image of the subtraction method is determined by subtracting the traditional image to the negative image. The subtraction coefficient is equal to α = 0.6. The size of the 3D image is set to 130μm × 40μm × 60μm. Figs. 3(a) and 3(b) show the 3D images of the conventional LSFM and the subtraction method respectively, while two cross-section planes of the traditional LSFM in zy and zx planes are indicated in Figs. 3(e), and 3(c), respectively, and Figs. 3(f) and 3(d) indicate two cross-section planes of the subtraction method in zy and zx planes, respectively. It can be clearly seen that the axial resolution of the subtraction method is higher than one of the traditional LSFM, which means that the subtraction method can be used to improve further axial resolution for LSFM. To analyze the enhancement of axial resolution, we measure the full width half maximum (FWHM) of fluorescent particles imaged along the z axis. The profiles along z axis obtained by both subtraction method and conventional LSFM are indicated in Fig. 3(g), where the positions of this fluorescent particle are indicated by white lines in Fig. 3(f) and Fig. 3(e). The FWHMs of traditional LSFM and subtraction method are equal to 2.61μm and 1.45μm, respectively.
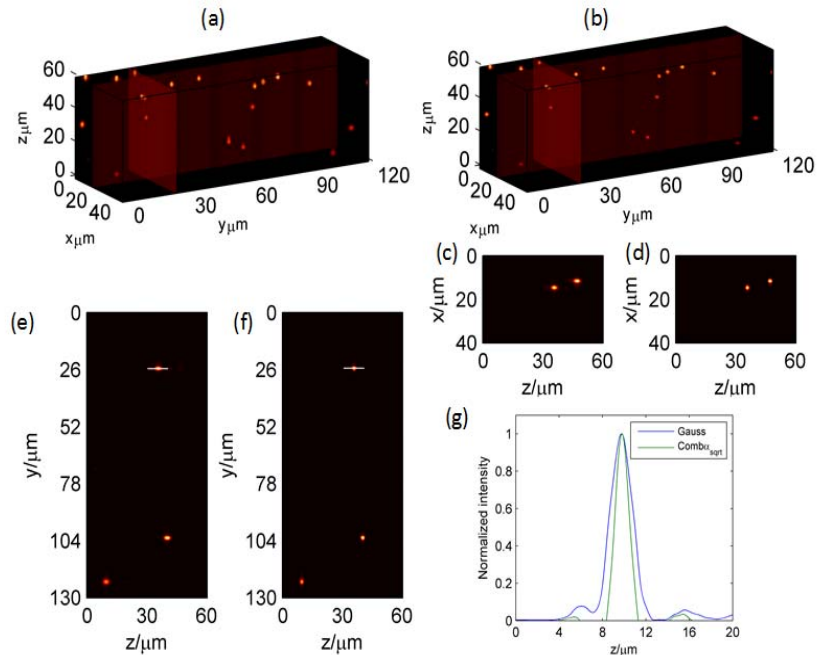
238

Fig. 3 Imaging result of 1μm diameter fluorescent particles. Fig. (a) is the 3D image of the traditional LSFM. Fig. (b) is the 3D image of the subtraction method.

IV. CONCLUSION

In summarize, we have introduced a novel combination using two light-sheets to improve axial resolution in LSM. Based on two images of both Gaussian light-sheet and negative light-sheet is captured, a new relationship between these two images is built to generate the higher axial-resolution image. The experimental result demonstrated that the better axial resolution of our method is achieved. In addition, this proposed approach can be applied to any optical microscopy techniques.

ACKNOWLEDGMENT

REFERENCES

[1] R. Han, Z. Li and Y. Jiang, J. Genet, "Recent advances in super-resolution fluorescence imaging and its applications in biology," Genomics. Vol. 40(12), pp. 583, 2013.

[2] J. Huisken et al., "Reconstruction of zebrafish early embryonic development by scanned light-sheet microscopy," Science. Vol. 322pp. 1065-1069, 2004,.

[3] G. Sena et al, "Quantitation of Cellular Dynamics in Growing Arabidopsis Roots with Light-sheet Microscopy," PloS ONE. Vol. 6, e21303, 2011.

[4] E. Fuchs, J. S. Jaffe, "Thin laser light-sheet microscope for microbial oceanography," Optics express. Vol. 10(2), pp. 145, 2002.

[5] C. Gohn-Kreuz and A. Rohrback, "Light needles in scattering media using self-reconstructing beams and the STED principle," Optica. Vol. 4(9), pp. 1134-1142, 2017.

[6] T. F. Holekamp, D. Turaga, T. E. Holy, "Fast three-dimensional fluorescence imaging of activity in neural populations by objective-coupled planar illumination microscopy," Neuron. Vol. 57(5), pp. 661-672, 2008.

[7] M. Friedrich and G. S. Harms, "Axial resolution beyond the diffraction limit of a sheet illumination microscope with stimulated emission depletion," J. Biomed. Opt. Vol. 20, pp. 106006, 2015.

[8] M. Friedrich et al, "STED-SPIM: Stimulated Emission Depletion Improves Sheet Illumination Microscopy Resolution," Biophys. J. Vol. 100, pp. L43-L45, 2011.

[9] A. Kumar, et al., "Dual-view plane illumination microscopy for rapid and spatially isotropic imaging," Protocol, Vol. 9(11), pp. 2555, 2014.

[10] P. J. keller et al., "Fast, high-contrast imaging of animal development with scanned light-sheet-based structured-illumination microscopy," Nat. Method, Vol. 7(8), pp. 637, 2010.

[11] P. Hoyer, et al., "Breaking the diffraction limit of light-sheet fluorescence microscopy by RESOLFT," PNAS, Vol. 113(13), pp. 3442–3446, 2016.

[12] B. Hu et al., "Improved contrast in inverted selective plane illumination microscopy of thick tissues using confocal detection and structured illumination," Bio. Opt. Express, Vol. 8(12), pp. 5546, 2017.

[13] B. J. Chang et al., "csiLSFM combines light-sheet fluorescence microscopy and coherent structured illumination for a lateral resolution below 100 nm," PNAS, Vol. 114(9), pp. 4869-4874, 2017.

[14] L. Gao, et al., "3D live fluorescence imaging of cellular dynamics using Bessel beam plane illumination microscopy," Protocol, Vol. 9(5), pp. 1083, 2014.

[15] U. Krzic, et al., "Multiview light-sheet microscope for rapid in to imaging," Nature methods, Vol. 9(7), pp. 730, 2012.

[16] S. Geissbuehler, etal., "Live-cell multiplane three-dimensional super-resolution optical fluctuation imaging," Nat. Commun, Vol. 5, pp. 5830, 2014.

[17] Q. Ma, et al., "Three-dimensional fluorescent microscopy via simultaneous illumination and detection at multiple planes," Sci. Rep, Vol. 6, pp. 31445, 2016.